Cell Cycle 12:7, 1091–1104; April 1, 2013; © 2013 Landes Bioscience

CDK4 inhibition restores G_1-S arrest in *MYCN*-amplified neuroblastoma cells in the context of doxorubicin-induced DNA damage

Sina Gogolin,[1] Volker Ehemann,[2] Gabriele Becker,[3] Lena M. Brueckner,[1] Daniel Dreidax,[1] Steffen Bannert,[1] Ingo Nolte,[4] Larissa Savelyeva,[1] Emma Bell[1] and Frank Westermann[1,*]

[1]Division of Tumor Genetics; German Cancer Research Center (DKFZ); Heidelberg, Germany; [2]Department of Pathology; University of Heidelberg; Heidelberg, Germany; [3]Clinical Cooporation Unit Pediatric Oncology; German Cancer Research Center (DKFZ); Heidelberg, Germany; [4]Small Animal Clinic; University of Veterinary Medicine Hannover; Hannover, Germany

Keywords: oncogene, RB1, TP53, cell cycle arrest, apoptosis

Abbreviations: doxo, doxorubicin

Relapse with drug-resistant disease is the main cause of death in *MYCN*-amplified neuroblastoma patients. *MYCN*-amplified neuroblastoma cells in vitro are characterized by a failure to arrest at the G_1-S checkpoint after irradiation- or drug-induced DNA damage. We show that several *MYCN*-amplified cell lines harbor additional chromosomal aberrations targeting p53 and/or pRB pathway components, including *CDK4/CCND1/MDM2* amplifications, *p16INK4A/p14ARF* deletions or *TP53* mutations. Cells with these additional aberrations undergo significantly lower levels of cell death after doxorubicin treatment compared with *MYCN*-amplified cells, with no additional mutations in these pathways. In *MYCN*-amplified cells CDK4 expression is elevated, increasing the competition between CDK4 and CDK2 for binding p21. This results in insufficient p21 to inhibit CDK2, leading to high CDK4 and CDK2 kinase activity upon doxorubicin treatment. CDK4 inhibition by siRNAs, selective small compounds or $p19^{INK4D}$ overexpression partly restored G_1-S arrest, delayed S-phase progression and reduced cell viability upon doxorubicin treatment. Our results suggest a specific function of $p19^{INK4D}$, but not $p16^{INK4A}$, in sensitizing *MYCN*-amplified cells with a functional p53 pathway to doxorubicin-induced cell death. In summary, the CDK4/cyclin D-pRB axis is altered in *MYCN*-amplified cells to evade a G_1-S arrest after doxorubicin-induced DNA damage. Additional chromosomal aberrations affecting the p53-p21 and CDK4-pRB axes compound the effects of MYCN on the G_1 checkpoint and reduce sensitivity to cell death after doxorubicin treatment. CDK4 inhibition partly restores G_1-S arrest and sensitizes cells to doxorubicin-mediated cell death in *MYCN*-amplified cells with an intact p53 pathway.

Introduction

Neuroblastoma is the most common solid extracranial tumor in early childhood, with clinical phenotypes varying from spontaneous regression or differentiation to relentless progression.[1-3] The 5-y survival rate of high-risk neuroblastoma patients remains below 35%,[4-6] which is mainly due to drug resistance of tumors and metastases after relapse. Characteristic for high-risk neuroblastomas is amplification of *MYCN* oncogene, which occurs in about 20% of all primary tumors and is associated with tumor progression or relapse and poor patient outcome.[7,8] The specific mechanisms of how MYCN interferes with cellular responses to drug treatment are still poorly understood. Studies showing that ectopic *MYCN* overexpression sensitizes neuroblastoma cells to p53-mediated apoptosis induced by irradiation or cytotoxic drugs[9-13] indicate that drug resistance of *MYCN*-amplified neuroblastoma cells may result from additionally altered expression of genes involved in DNA damage response.

Cellular DNA damage response after irradiation or drug exposure involves different biological processes, including cell cycle arrest, apoptosis, differentiation and DNA repair. The p53 and pRB tumor suppressors are both important to prevent replication of cells with damaged DNA, implying that the clinical efficacy of chemotherapeutic drugs or irradiation will be influenced by both p53 and pRB status in the target tumor. Following drug-induced DNA damage, p53 protein is upregulated, leading to transcriptional activation of a large number of target genes, including *BAX* and *CDKN1A* (*p21CIP1*). p21, in turn, binds to CDK2 to inhibit its function and cause G_1 cell cycle arrest. Pro-apoptotic genes activated by p53, such as *BAX*, may trigger cell death when DNA damage cannot be repaired. Functional pRB is also essential for G_1 arrest following irradiation or drug treatment.[14,15] This is supported by $RB1^{-/-}$ mouse embryo fibroblasts

*Correspondence to: Frank Westermann; Email: f.westermann@dkfz.de
Submitted: 11/23/12; Revised: 02/22/13; Accepted: 02/23/13
http://dx.doi.org/10.4161/cc.24091

failing to arrest in G_1-S despite p53-*p21CIP1* activation.[16] Loss of pRB does not interfere with either p21 induction or inhibition of CDK2 activity in response to γ-irradiation, suggesting that pRB acts downstream of p21 during p53-dependent G_1 arrest.[17] Intriguingly, drug-induced DNA damage causes *RB1*$^{+/+}$ and *RB1*$^{+/-}$ fibroblasts to arrest but induces apoptosis in *RB1*$^{-/-}$ fibroblasts. From these findings, it has been hypothesized that the susceptibility of tumor cells—as opposed to normal cells—to undergo p53-dependent apoptosis arises from their inability to enforce a pRB-dependent cell cycle arrest. Consequently, alterations of the p53 pathway, including *TP53* mutations, would mark a switch to a chemotherapy-resistant tumor. Although frequent in other human cancers,[18] *TP53* mutations occur in less than 2% of primary neuroblastomas. *MDM2* amplification and loss of *p14ARF*, which result in inhibition of p53 functions, occasionally occur in relapse tumors and neuroblastoma cell lines established from tumors following chemotherapy.[19-21] DNA damage response in p53 wild-type neuroblastoma cells seems to be determined by MYCN expression level.[22] MYCN regulates several components of the p53-p21 axis.[9,13,23-26] MYCN transcriptionally activates both *TP53* and the p53 inhibitor *MDM2* and suppresses *p21CIP1* transcription. However, p53 remains transcriptionally active and induces p21 after irradiation- or drug-induced DNA damage in *MYCN*-amplified neuroblastoma cells.[27] Despite this, *MYCN*-amplified neuroblastoma cells fail to induce functional G_1 arrest,[12,27-29] indicating a failure downstream p21 signaling to be involved in the impaired cell cycle arrest. Indeed, a later study found that the level of p21 induction after DNA damage is significantly lower in *MYCN*-amplified compared with *MYCN*-single-copy cells.[12] Analysis of resistance to different chemotherapeutic agents in several neuroblastoma cell lines established at different points of therapy revealed that most cell lines deriving from progressive tumors or relapses were highly resistant to doxorubicin.[30] Doxorubicin is commonly used for treatment of high-risk neuroblastomas. It induces DNA damage through different mechanisms, including DNA intercalation, topoisomerase II inhibition and free radical formation,[31] which, similar to irradiation-induced DNA damage, should result in G_1 cell cycle arrest and apoptosis.

We have previously established that MYCN upregulates the CDK4/cyclin D1 complex in high-risk neuroblastomas and particularly *MYCN*-amplified tumors.[24] A study using c-myc-3'RR/p53$^{+/-}$ and c-myc-3'RR/Cdk4^{R24C} (a Cdk4-Arg24Cys mutation that prevents binding of all four INK4 members to Cdk4) mouse models revealed that both mice developed MCL-like lymphomas with similar gene expression profiles that differ only in those related to the p53 or Cdk4^{R24C} mutation.[32] This suggests that the expression level of MYCN and the functional status of p53 and CDK4 may play a role in tumorigenesis, including neuroblastoma. We hypothesized here that highly abundant CDK4/cyclin D1 may weaken the G_1 checkpoint after doxorubicin-induced DNA damage in *MYCN*-amplified neuroblastoma cells, and investigated whether amplified *MYCN* and/or chromosomal aberrations of pRB pathway members (e.g., *CDK4* or *CCND1* amplification, *p16-INK4A* deletion) are associated with an attenuated G_1 arrest after drug-induced DNA damage in neuroblastoma cell lines. Because CDK4- and CDK2-containing complexes both bind p21, we tested whether highly abundant CDK4/cyclin D1 complexes compete with CDK2-containing complexes for newly induced p21 after drug-induced DNA damage. To test whether CDK4 inhibition can restore a functional G_1 arrest and sensitize cells to drug-induced death, we inhibited CDK2 and CDK4 using small-molecule inhibitors, shRNA/siRNA methodology and tetracycline-inducible cell models to modulate p19^{INK4D} and p16^{INK4A} expression.

Results

Deregulated MYCN impairs cell cycle arrest after drug-induced DNA damage. To define the role of MYCN after doxorubicin (doxo)-induced DNA damage, we used two MYCN regulatable neuroblastoma cell models, one having a *MYCN*-amplified genetic background and the other, single-copy *MYCN*. Cell cycle distribution and cell death were analyzed using flow cytometry in control or doxo-treated cells. *MYCN*-amplified IMR5/75-C2 stably express a tetracycline-inducible *MYCN* shRNA that, upon induction, reduced MYCN protein to approximately 35%.[33] Untreated IMR5/75-C2 cultures with high endogenous MYCN expression showed higher numbers of cycling cells (S and G_2/M) compared with IMR5/75-C2 expressing the *MYCN* shRNA, indicating that even reducing MYCN protein levels to ~35% has a robust impact on cell cycle distribution (**Fig. 1A**). Doxo treatment further depleted uninduced (MYCN-expressing) IMR5/75-C2 cultures of $G_0/_1$ phase cells. Reduction of MYCN by inducing the *MYCN*-targeting shRNA in these cultures restored G_1 arrest after doxo treatment and diminished the G_2/M fraction by 2.5-fold (**Fig. 1A**). The sub-G_1 fraction, indicative of apoptosis, after doxo treatment was not significantly different between IMR5/75-C2 cultures expressing low or high MYCN (33.8% ± 0.5 and 34.6% ± 0.4, respectively) (**Fig. 1B**).

We compared the findings in IMR5/75-C2 with those in SH-EP-*MYCN* (TET21N), which stably express a tetracycline-regulatable *MYCN* transgene allowing MYCN induction by removal of tetracycline from the culture medium.[34] Untreated SH-EP-*MYCN* cultures expressing the *MYCN* transgene contained higher numbers of cycling cells (S and G_2/M) than cultures without *MYCN* transgene expression. Doxo treatment of MYCN-expressing SH-EP-*MYCN* cultures further reduced the $G_0/_1$ fraction by 7.4% of untreated cultures, whereas doxo treatment did not affect the fraction of cells in $G_0/_1$ in SH-EP-*MYCN* cultures with an inactive *MYCN*. Doxo treatment reduced the fraction of SH-EP-*MYCN* cells in S-phase and enriched the fraction of SH-EP-*MYCN* cells in the G_2/M phase regardless of whether the *MYCN* transgene was activated or not (**Fig. 1A**). The sub-G_1 fraction of either untreated or doxo-treated SH-EP-*MYCN* cells overexpressing MYCN was also higher than in cultures without the active *MYCN* transgene (**Fig. 1B**). These experiments demonstrate that ectopic MYCN expression in neuroblastoma cells with a single-copy *MYCN* genetic background does not fully recapitulate the response to doxo in *MYCN*-amplified cells. This suggests that the higher MYCN dosage together with

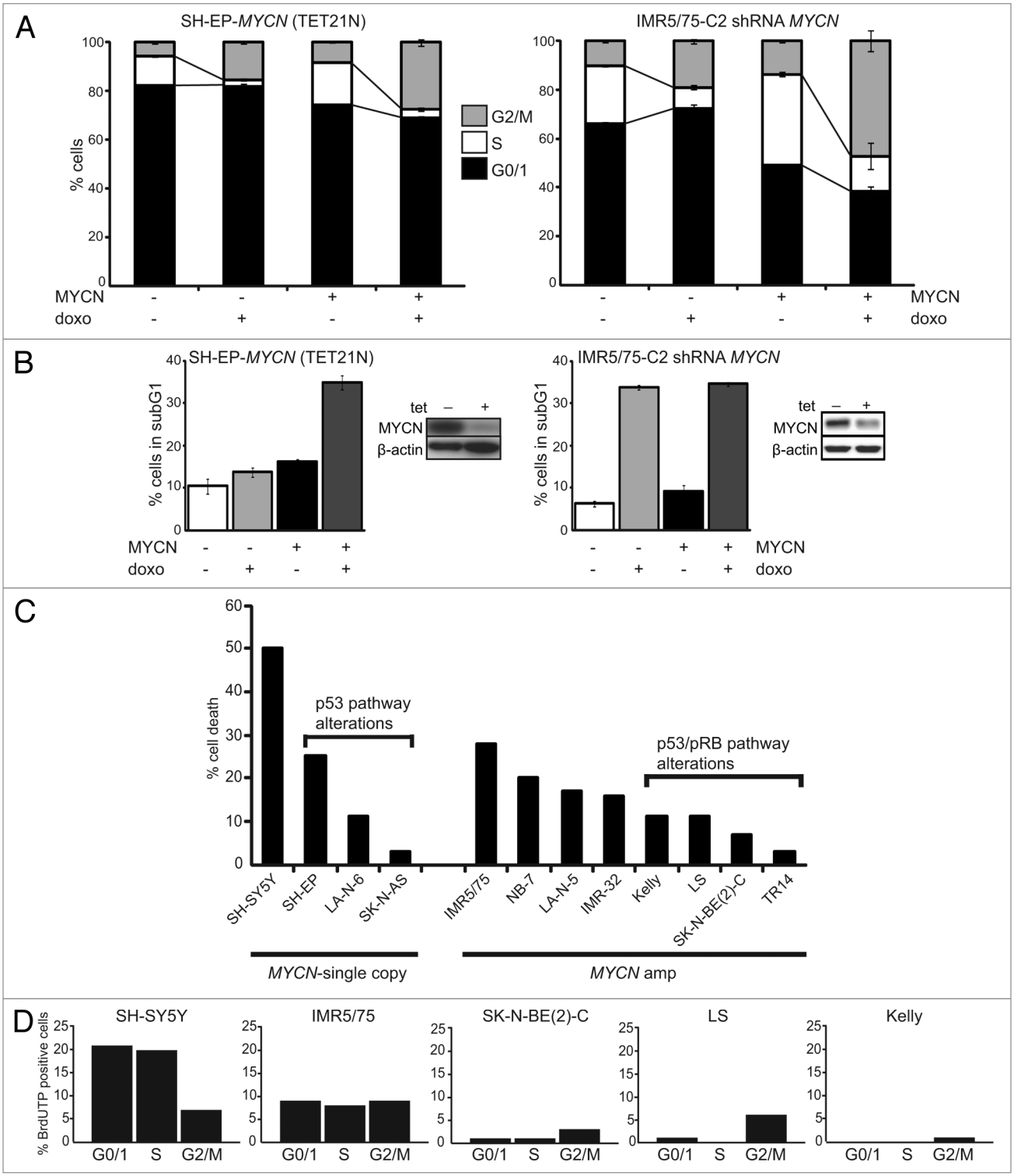

Figure 1. Amplified *MYCN* and additional chromosomal aberrations impair drug-induced DNA damage response in neuroblastoma cells. SH-EP-*MYCN* cells were treated with tetracycline to suppress *MYCN* transgene expression. IMR5/75-C2 cells were treated with tetracycline to induce the shRNA targeting *MYCN* (= MYCN-). Doxo was added to the culture medium 48 h later after tetracycline addition. Cell cycle (**A**) and cell death (**B**) were analyzed using flow cytometry 48 h after doxo addition. Data are presented as mean ± SD of triplicates. (**B**) Also shows a western blot of MYCN knockdown 48 h after addition of tetracycline to the media. (**C**) Cell death was analyzed 48 h after doxo treatment using flow cytometry (sub-G_1 fractions). Shown here is the cell death enhancement (% sub-G_1 cells upon doxo treatment – % sub-G_1 cells of untreated cultures). Data are presented as mean ± SD of triplicates. (**D**) Cells were treated with doxo, 48 h later fixed and double stained with propidium iodide and BrdUTP to detect DNA breaks. Data shows one representative experiment.

Table 1. Drug-induced DNA damage response of neuroblastoma cell lines

No.	DNA damage response group	Cell line	$G_0/_1$ changes after doxo (%)	S changes after doxo (%)	G_2/M enrichment (fold)	MYCN/MYC status	pRB pathway alterations	p53 pathway alterations	Other genetic alterations
1	response group 1	NB-7	−7	−95	4.0	*MYCN* amp	1	2	1p del; 17q gain
2		TR14	−11	−37	3.7	*MYCN* amp	CDK4 amp (dmins)	MDM2 amp (dmins)	1p del; 17q gain
3		SK-N-BE(2)-C	−11	−78	3.9	*MYCN* amp	1	TP53 mut	1p del; 17q gain
4		IMR-32	−16	−67	3.6	*MYCN* amp	1	2	1p del; 11q del; 17q gain
5		IMR5/75	−22	−100	4.1	*MYCN* amp	1	2	1p del; 11q del; 17q gain
6		Kelly	−34	−100	11.1	*MYCN* amp	1	TP53 mut	1p del; 11q del; 17q gain
7		SK-N-AS	−60	−100	5.0	high MYC	1	TP53 mut	1p del; 11q del; 17q gain
8		NGP	−88	−77	10.0	*MYCN* amp	CDK4 amp (HSR)	MDM2 amp (HSR)	t(1p); 11q del; 17q gain
9		LS	−90	−99	4.7	*MYCN* amp	CDK4 amp (HSR); CCND1 amp (HSR)	MDM2 amp (HSR)	1q gain; 17q gain
10	response group 2	LA-N-6	−14	−2	4.2	high MYC	p16-INK4A del; CCDN1 dupl	p14ARF del	1p del; 11p del; 14q gain; 17q gain
11		LA-N-5	−14	33	1.5	*MYCN* amp	1	2	1p del; 17q gain
12	response group 3	SH-EP	4	−92	2.7	high MYC	p16-INK4A del	p14ARF del	del (14); 17q gain
13		SJ-NB-12	−4	−91	7.4	*MYC* amp	p16-INK4A del	p14ARF del	1p del; 17q gain
14	response group 4	SH-SY5Y	−6	−4	1.5	high MYC	1	2	del (14); 17q gain
15	Ewing sarcoma	SK-N-MC	26	0	0.04	*MYC* amp	n.d.	*TP53* mut	*EWS-FLi1* gene fusion

Measure for G_1 or S arrest after drug-induced DNA damage response is given by the change of cells in $G_0/_1$ or S phase after doxo treatment compared with the untreated control; G_2/M enrichment, ratio G_2/M doxo/G_2/M untreated; all experiments were done in triplicate; [1]copy number status of *p16-INK4A*, *CDK4/6*, *RB1*, *CCND1* normal; [2]copy number status of *p14ARF*, *MDM2*, *TP53* normal; amp, amplification; dupl, duplication; del, deletion; t(1p), reciprocal 1;15 translocation; high, high expression; mut, mutation; dmins, double minutes; HSR, homogeneously staining region; n.d., not defined.

the cellular genetic background establishes the impaired DNA damage response in *MYCN*-amplified cells.

MYCN amplification and chromosomal aberrations of p53 and/or pRB pathway members impaired doxo-induced DNA damage response in neuroblastoma cells. We next investigated whether genetic aberrations affecting the p53 and/or pRB pathways in addition to *MYCN* amplification are involved in establishing the impaired drug-induced DNA damage response. We analyzed the effect of doxo treatment on the cell cycle and cell death in 13 well-characterized neuroblastoma cell lines and a primary neuroblastoma short-term culture (NB-7) using flow cytometry (**Table 1**; **Fig. S1**). The percent change in the fraction of cells in the $G_0/_1$ and S phases and the fold-change of the G_2/M phase cell enrichment were determined after doxo treatment compared with untreated control cultures. Together these values were used to define characteristic neuroblastoma cell responses to DNA damage and separate the cell lines into defined DNA damage response groups (**Table 1**). Eight of nine tested *MYCN*-amplified neuroblastoma cell lines showed prominent reduction of $G_0/_1$ and S phase cells and massive enrichment of G_2/M phase cells after doxo treatment (response group 1). Only *MYCN*-amplified LA-N-5 showed S phase cell enrichment associated with reduction of $G_0/_1$ phase cells (response group 2). The failure of most *MYCN*-amplified cell lines to arrest in G_1 and/or S phase after doxo treatment was associated with additional chromosomal aberrations of p53 and/or pRB pathway members. For instance, NGP and LS both harbor amplified *MYCN*, *CDK4* and *MDM2* and showed the most pronounced $G_0/_1$ fraction reduction and G_2/M cell enrichment after doxo treatment (**Fig. S1**, LS additionally harbor an amplified *CCND1* gene, and **Fig. S2**). Neuroblastoma cell lines lacking amplified *MYCN* responded variably to drug-induced DNA damage, and the response was dependent on chromosomal aberrations affecting p53 and/or pRB pathway members. SK-N-AS harbors a *TP53* mutation,

and showed a prominent reduction of $G_0/_1$ and S phase cells and G_2/M fraction enrichment (response group 1) after doxo treatment, similar to *MYCN*-amplified cells. LA-N-6, with a *p16-INK4A/p14ARF* deletion and a *CCND1* duplication had a similar DNA damage response phenotype (response group 2) to *MYCN*-amplified LA-N-5, but lacked S phase cell enrichment (**Table 1**; **Fig. S2**). SH-EP, a subclone of SK-N-SH that harbors a *p16INK4A/p14ARF* deletion, showed an intermediate DNA damage response phenotype (response group 3) with no change in the $G_0/_1$ fraction and a reduced S phase fraction. This is probably due to deleted *p16INK4A/p14ARF*, because another subclone of SK-N-SH with normal *p16INK4A/p14ARF,* SH-SY5Y (response group 4), did not show a prominent change in the S phase fraction after doxo treatment. In summary, these results demonstrate that, besides amplified *MYCN*, chromosomal aberrations of p53 and/or pRB pathway members impair G_1-S cell cycle arrest and lead to G_2/M cell enrichment.

We quantified the enhancement of cell death by doxo treatment by calculating the difference between the sub-G_1 fractions of doxo-treated and untreated cultures (**Fig. 1C**). The strongest enhancement of cell death occurred in *MYCN*-single-copy SH-SY5Y. Doxo treatment induced less cell death in the other SK-N-SH subclone, SH-EP, and two other *MYCN*-single-copy cell lines, which harbor either a *p16INK4A/p14ARF* deletion (LA-N-6) or mutant *TP53* (SK-N-AS). *MYCN*-amplified cell lines without additional alterations of p53 pathway components underwent modest levels of cell death but less compared with *MYCN*-single-copy SH-SY5Y. *MYCN*-amplified neuroblastoma cell lines with chromosomal aberrations of p53 pathway members (either *p14ARF* deletion, *MDM2* amplification or *TP53* mutation) exhibited significantly lower enhancement of cell death ($p = 0.014$, Wilcoxon test) upon doxo treatment. Together, this indicates that impairing p53 antagonizes the pro-apoptotic functions of MYCN.

We further investigated whether doxo-induced cytotoxicity is dependent on the capability of neuroblastoma cells to arrest in G_1-S. To determine the cell cycle phase of cell death induction, DNA breaks in $G_0/_1$, S and G_2/M phases were assessed using a double staining with propidium iodide and BrdUTP after doxo treatment. *MYCN*-single-copy SH-SY5Y were used as a reference, because doxo treatment induced cell death most strongly in this cell line. BrdUTP-positive SH-SY5Y cells were predominantly observed in the $G_0/_1$ and S phases. In the *MYCN*-amplified cell line IMR5/75, which has no additional alterations targeting the p53 and pRB pathway, BrdUTP-positive cells were assessed equally in the $G_0/_1$, S and G_2/M phases. Contrastingly, only few BrdUTP-positive cells were observed in the $G_0/_1$ and S phases in the three *MYCN*-amplified cell lines that harbor additional alterations of p53 and/or pRB pathway components (**Fig. 1D**). We also observed that the number of DNA breaks differed in the four *MYCN*-amplified cell lines, which was dependent on additional chromosomal aberrations of p53 and/or pRB pathway members. Thus, SK-N-BE(2)-C, Kelly and LS, harboring either a *TP53* mutation or amplification of *CDK4* and *MDM2*, showed less BrdUTP-positive cells compared with IMR5/75, which has none of the investigated additional chromosomal aberrations besides amplified *MYCN*. Collectively, this demonstrates the role of chromosomal aberrations in p53 and/or pRB pathway members, including *CDK4*/*CCND1* and *MDM2* amplifications, *p16INK4A/p14ARF* deletion or *TP53* mutation, in impairing G_1-S arrest and cell death after doxo treatment.

Competitive binding of p21 to CDK4 and CDK2 complexes results in high CDK4 and CDK2 kinase activities in *MYCN*-amplified neuroblastoma cells after doxo-induced DNA damage. Deregulated *MYCN* increases the activity of the G_1 cell cycle kinases, CDK4 and CDK2, by transcriptionally activating *CDK4*[24] and suppressing *p21CIP1*.[23] We hypothesized that impaired G_1 arrest after doxo-induced DNA damage could be associated with high G_1 cell cycle kinase activity. CDK2 and CDK4 activity was assessed in untreated and doxo-treated cell lines with various *MYCN* or *MYC* genetic backgrounds, including single-copy *MYCN* (SH-SY5Y and SH-EP), amplified *MYCN* (IMR-32, Kelly and LS) and amplified *MYC* (SK-N-MC Ewing sarcoma cell line). The SK-N-SH subclone, SH-SY5Y, showing almost unchanged $G_0/_1$ and S phase fractions and the highest level of cell death after doxo treatment, exhibited the lowest CDK2 and CDK4 activity in untreated and doxo-treated cultures of all cell lines that we analyzed. The other SK-N-SH subclone, SH-EP, which is *p16INK4A/p14ARF* deleted, exhibited higher CDK4 and CDK2 activities than SH-SY5Y, which could be due to the lack of $p16^{INK4A}$ and $p14^{ARF}$ expression. CDK4 activity tended to decrease after doxo treatment in all three *MYCN*-amplified cell lines, but still remained higher than in untreated SH-SY5Y. CDK2 activity decreased in only one out of three *MYCN*-amplified cell lines (IMR-32) after doxo treatment, but remained higher than in both SH-SY5Y and SH-EP subclones with single-copy *MYCN* (**Fig. 2A**). Similar to CDK4, CDK1 activity also remained high in *MYCN*-amplified neuroblastoma cell lines after doxo treatment (**Fig. S3**). These results indicate that after doxo treatment the activity of cell cycle kinases is only minimally affected in *MYCN*-amplified neuroblastoma cells.

Following drug-induced DNA damage, activity of CDK4 and CDK2 is controlled by activation of the p53-p21 axis, and also independently of p53, through proteolysis of cyclin D1 releasing p21 from the CDK4/cyclin D1 complex, which, in turn, inactivates CDK2.[35] We evaluated the relative amounts of p21 in G_1 cell cycle kinase complexes before and after doxo treatment in two *MYCN*-single-copy, four *MYCN*-amplified neuroblastoma cell lines and the SK-N-MC Ewing sarcoma cell line using co-immunoprecipitation with antibodies against CDK4 and CDK2. All cell lines harboring *TP53* mutations, which included Kelly, SK-N-BE(2)-C and SK-N-MC, lacked p21 expression independent of doxo treatment (**Fig. 2B**). Generally, p21 levels were low in untreated neuroblastoma cells. Thus, complexes precipitated with antibodies against either CDK4 or CDK2 in most untreated neuroblastoma cell lines contained barely detectable amounts of p21. With such low levels of available p21, only a small pool can be expected to shift from CDK4- to CDK2-containing complexes upon doxo treatment. Doxo treatment induced p21 expression only in p53 wild-type neuroblastoma cells. Induction of p21 after doxo treatment was less in all cell lines that also harbored amplified *MYCN*, namely IMR-32 and LS (**Fig. 2B**),

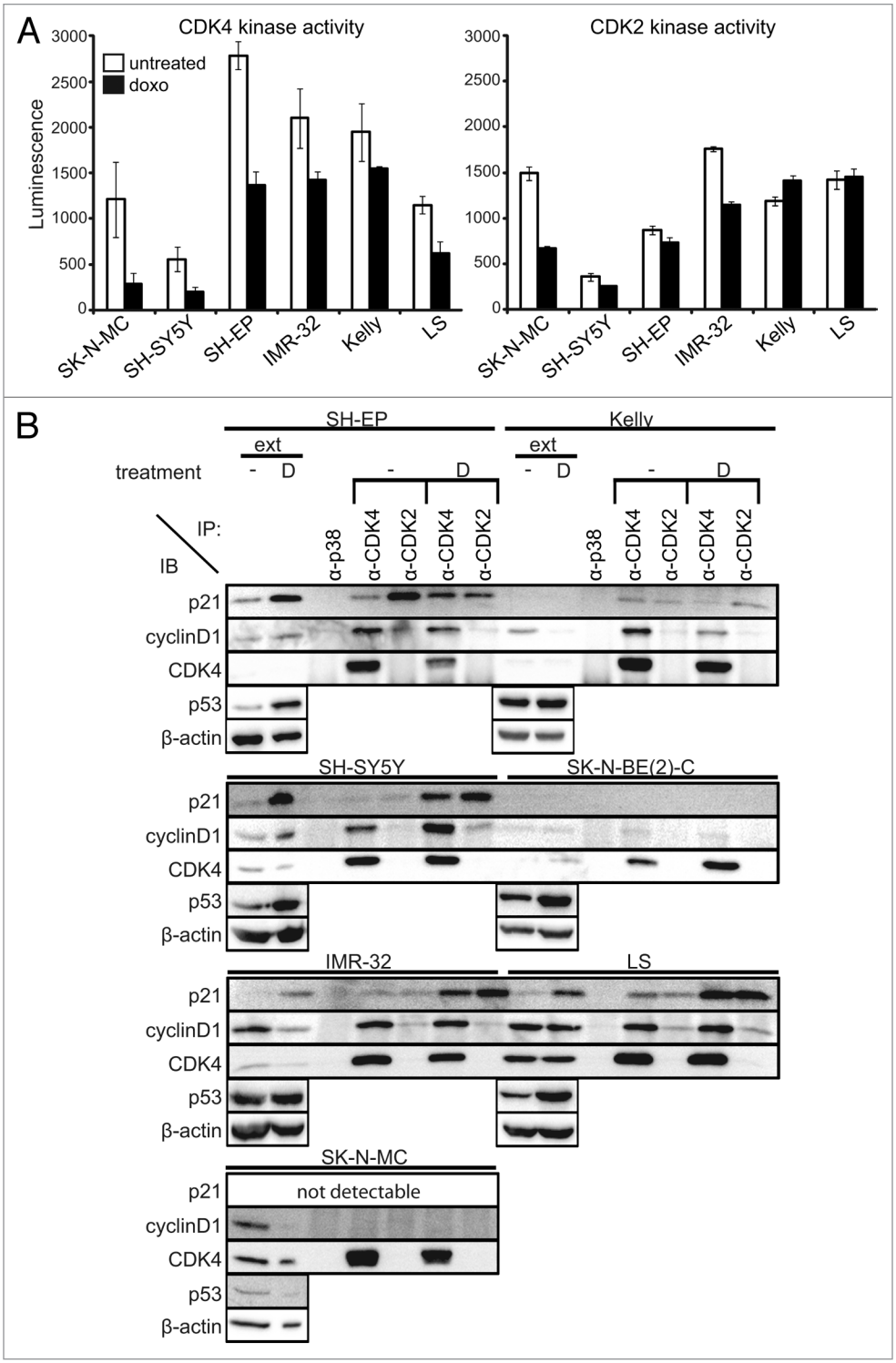

Figure 2. High CDK4 and CDK2 activity after doxorubicin treatment of *MYCN*-amplified cells. (**A**) CDK4 and CDK2 activity were analyzed 48 h after treatment using RB and histone 1 as substrates, respectively. Luminescence directly correlates to the amount of produced ADP, indicative for kinase activity. Data are presented as mean ± SD of duplicates. (**B**) Whole-cell protein extracts were prepared 48 h after doxo treatment and immunoprecipitated with anti-CDK4, anti-CDK2 or control anti-p38 antibodies. Then, 50 μg of whole-cell protein extracts (ext) and 500 μg of the immunoprecipitates (IP) were separated on 12.5% SDS-PAGE. β-actin was used as loading control for whole-cell protein extracts.

which is consistent with lower p21 levels observed after irradiation in *MYCN*-amplified compared with *MYCN*-non-amplified cell lines.[12] Following doxo treatment, p21 was distributed in both CDK4- and CDK2-containing complexes. Overall CDK2 activity remained high after doxo treatment in *MYCN*-amplified, *TP53*-wild-type cells, despite a substantial amount of p21 in

CDK2-containing complexes. Sequestration of p21 produced in response to DNA-damaging drugs away from CDK2 complexes into highly abundant CDK4/cyclin D1 complexes may result in unaltered CDK2 activity in the *MYCN*-amplified neuroblastoma cells.

CDK4 inhibition partially restores G_1-S cell cycle arrest and reduces viability after drug treatment in *MYCN*-amplified cells. To further investigate the effects of CDK4 and CDK2 activity on drug-induced cell cycle arrest in *MYCN*-amplified cells, CDK4 and/or CDK2 were selectively inhibited in combination with doxo treatment, and cell cycle changes were assessed using flow cytometry. Transient transfection of two *CDK4* siRNAs achieved knockdown efficiencies of 76% and ~96% in LS and SK-N-BE(2)-C, respectively, at the protein level (**Fig. 3A**). CDK4 knockdown increased the $G_0/_1$ fraction and decreased the number of cells in G_2/M phase in both untreated and doxo-treated cultures compared with non-transfected or with control siRNAs transiently transfected cells (**Fig. 3B**; **Fig. S4**). To validate the effect of CDK4 inhibition, we treated 12 neuroblastoma cell lines previously characterized in **Table 1** with a CDK4-specific small-molecule inhibitor (RO050124), which has been shown to delay $G_0/_1$ in cells with functional pRB.[36] Combined RO050124 and doxo treatment increased the $G_0/_1$ and S phase fractions in nine and six cell lines, respectively, and reduced the G_2/M fraction in 11 cell lines compared with cultures treated only with doxo (**Fig. 3C**, results are shown for SK-N-BE(2)-C, LS, Kelly and IMR-32). This confirmed our results obtained by transient silencing of CDK4 using siRNAs. We next tested whether CDK4 inhibition by RO050124 was capable of enhancing the inhibitory effect of doxo on neuroblastoma cell viability using the alamarBlue assay. Here, we focused on *MYCN*-amplified neuroblastoma cell lines harboring additional aberrations of p53 pathway members, namely *TP53*-mutant SK-N-BE(2)-C and *MDM2*-amplified LS, which responded poorly to doxo treatment with cell death responses of only 7% and 11%, respectively (**Table 1**). Combined treatment achieved at least an additive effect on viability reduction for both cell lines compared with the doxo or RO05012 treatment alone (**Fig. 3D**). To test whether this inhibitory effect on viability in these cells after CDK4 inhibition results from G_1-S cell cycle arrest or also from cell death, we assessed the sub-G_1 fraction of *TP53*-mutant SK-N-BE(2)-C, and *MDM2*-amplified LS after combined treatment with doxo and the CDK4 inhibitor, RO050124. Sensitization to cell death could not be observed in these cell cultures. Inhibition of CDK4 in two other cell lines that are characterized by an impaired p53 pathway, Kelly and TR14, did also not sensitize for doxo-induced cell death (**Fig. S5**), indicating that the combinatory treatment promotes a G_1-S arrest as opposed to cell death, at least in cell lines with p53 pathway aberrations.

We also analyzed the effect of CDK2 inhibition on cell cycle arrest after drug-induced DNA damage using siRNA-mediated silencing. CDK2 activity has been previously shown to be required for irradiation-induced DNA damage response at least in (1) untransformed human telomerase-expressing retinal pigment epithelial cells, RPE-hTERT; (2) the human colon carcinoma cell line, HCT116; and (3) NBS-T cells deriving from a patient with Nijmegen Breakage Syndrome.[37] Three *MYCN*-amplified cell lines were transiently transfected with four siRNAs targeting different sequences in the *CDK2*-coding region. These siRNAs achieved knockdown efficiencies between 50–86% in all three cell lines on the protein level. The most effective knockdown was achieved by siRNA#2 (72–86% knockdown, **Fig. 4A**). CDK2 knockdown increased the $G_0/_1$ fraction and decreased the number of cells in G_2/M phase in both untreated and doxo-treated cultures compared with non-transfected or with control siRNAs transiently transfected cells. In contrast to CDK4 inhibition, CDK2 knockdown did not significantly alter the S phase fraction in both untreated and doxo-treated cultures (**Fig. 4B**; **Fig. S6**). We also assessed drug-induced cell cycle arrest in the *MYCN*-amplified IMR-32 model that stably expresses a tetracycline-inducible *CDK2* shRNA (IMR-32-*CDK2*shRNA).[38] Induction of the *CDK2*-targeting shRNA achieved CDK2 knockdown of > 95% at the protein level (**Fig. 4C**). CDK2 knockdown in combination with doxo treatment increased the $G_0/_1$ fraction by 22.2-fold and prevented G_2/M cell enrichment. CDK4 inhibition using RO050124 increased the $G_0/_1$ fraction by 10.4-fold. Combined CDK2 and CDK4 inhibition using siRNA methodology and the small-molecule compound RO050124 further increased the $G_0/_1$ fraction (**Fig. 4C**). To test whether CDK2 and/or CDK4 inhibition sensitizes for doxo-induced cell death in cells with functional p53 signaling, we also assessed the sub-G_1 fraction in IMR-32-*CDK2*shRNA and parental IMR-32 cells. CDK4 inhibition by RO050124 or siRNA-mediated knockdown modestly increased doxo-induced cell death in IMR-32-*CDK2*shRNA cells expressing high levels of CDK2 and parental IMR-32 cells (**Fig. 4D and E**). Intriguingly, additional knockdown of CDK2 by shRNA induction reduced the sub-G_1 fraction in doxo-treated IMR-32-*CDK2*shRNA cultures compared with cells expressing high CDK2 levels. Moreover, the sensitizing effect of the CDK4 inhibitor, RO050124, to doxo was reversed by simultaneous CDK2 knockdown in IMR-32-*CDK2*shRNA cells (**Fig. 4D**). CDK2 inhibition did also not sensitize for doxo-induced cell death in neuroblastoma cells with an impaired p53 pathway (**Fig. 4F**). Taken together, these experiments demonstrate that either CDK4 or CDK2 inhibition restores doxo-induced G_1 cell cycle arrest in *MYCN*-amplified neuroblastoma cells, but only CDK4 inhibition further increases the S phase upon DNA damage. CDK4 inhibition yields a cooperative cytostatic effect with doxo independent of functional p53 and further sensitizes for doxo-induced cell death but only in cell lines without additional alterations targeting the p53 pathway.

***p19^{INK4D}*, but not *p16^{INK4A}*, abrogates cell cycle progression in *MYCN*-amplified neuroblastoma cells and sensitizes for cell death after drug-induced DNA damage.** To further address the role of CDK4 in impairing drug-induced cell cycle arrest, we focused on the activity and protein expression status of CDK4 downstream targets in the pRB-E2F signaling pathway. Phosphorylation status of pRB was determined using western blotting after doxo treatment of three *MYCN*-amplified cell lines [IMR5/75, SK-N-BE(2)-C and LS] and the SH-SY5Y *MYCN*-single-copy cell line. We found an increased phosphorylation of pRB on its CDK4-specific binding site Ser780[39] after

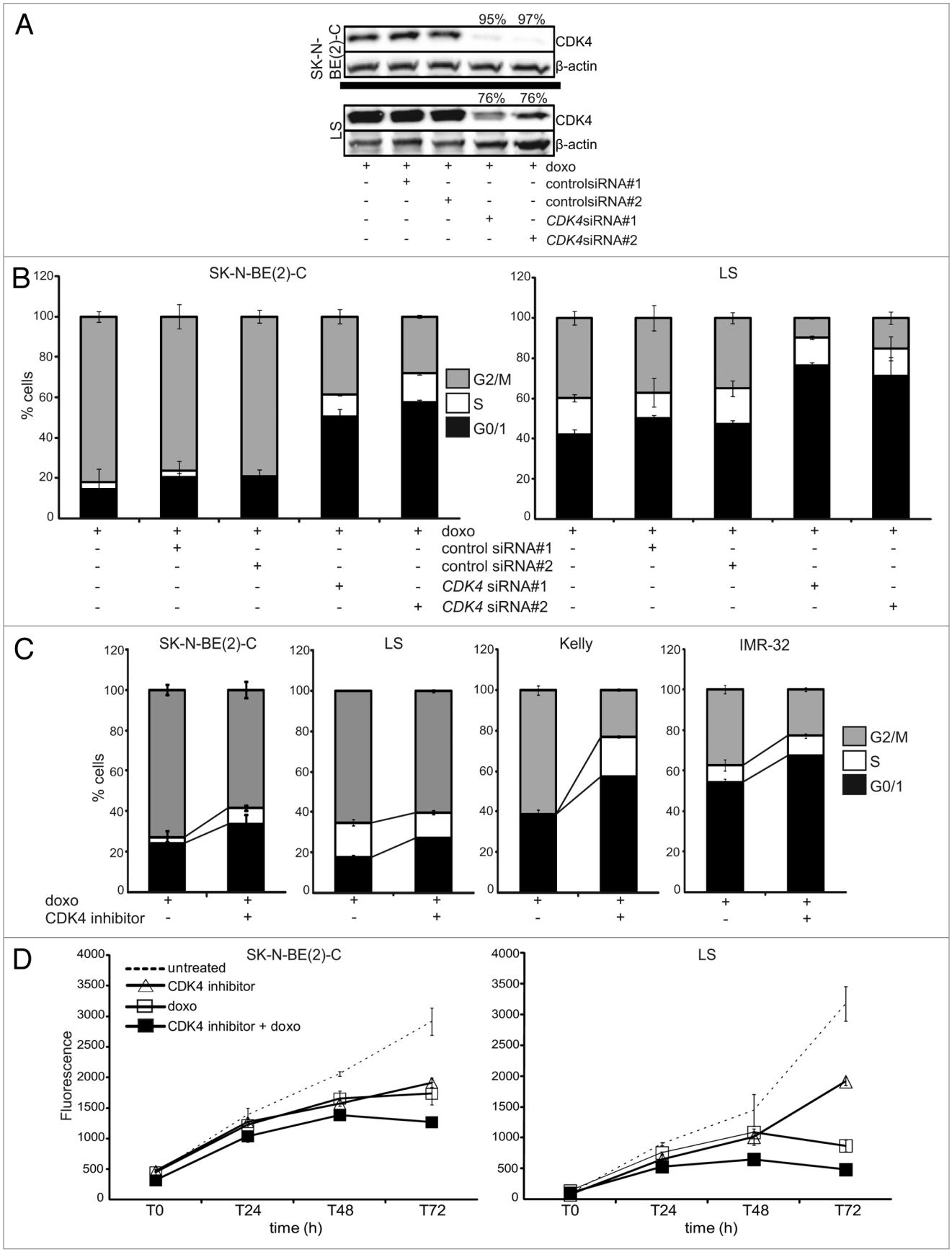

Figure 3. For figure legend, see page 1099.

Figure 3 (See opposite page). CDK4 inhibition partially restores G_1-S arrest and reduces cell viability upon drug treatment in *MYCN*-amplified cells. (**A and B**) Cells were transiently transfected with one of two different *CDK4* siRNAs or one of two unrelated control siRNAs, then treated with doxo 24 h after transfection. Knockdown efficacies of both *CDK4* siRNAs (%) are shown in the western blot (**A**), in addition to flow cytometric cell cycle analyses performed 48 h after doxo treatment (**B**). (**C**) Flow cytometric cell cycle analyses after 48 h of treatment with doxo and/or the CDK4 inhibitor, RO0505124. (**D**) Cell viability was assessed after doxo and/or RO0505124 treatment at the indicated time points using the alamarBlue assay. Data shown in (**B–D**) are presented as mean ± SD of triplicates.

doxo treatment in *MYCN*-amplified cells. Doxo treatment also resulted in strong expression of the SKP2 ubiquitin ligase, an inhibitor of p21 and p27 and a prototypic E2F target, in *MYCN*-amplified cells. In contrast, pRB phosphorylation and SKP2 expression decreased in *MYCN*-single-copy SH-SY5Y cells upon doxo treatment (**Fig. 5A**). Together, this suggests that high CDK4 activity in a *MYCN*-amplified cell makes the cell refractory to drug-induced DNA damage and favors cell cycle progression at least partly through pRB hyperphosphorylation. To further investigate whether CDK4 inhibition could prevent pRB Ser780 phosphorylation and restore drug-induced cell cycle arrest, we used the CDK4-specific small-molecule inhibitor, RO050124. In addition, we generated neuroblastoma cell lines stably expressing tetracycline inducible constructs for the two endogenous CDK4 inhibitors, *p16-INK4A* or *p19-INK4D*.[40-42] RO050124 treatment, induction of *p19-INK4D* or *p16-INK4A* prevented pRB Ser780 phosphorylation, but only CDK4 inhibition through RO050124 or *p19-INK4D* induction decreased SKP2 expression in *MYCN*-amplified cells after doxo treatment (**Fig. 5A and B**). Flow cytometric analysis revealed that the combination of *p19-INK4D* induction with doxo treatment in *MYCN*-amplified IMR5/75 almost doubled the $G_0/_1$ fraction, similar to the effect of CDK4 inhibition using RO050124 or siRNAs, compared with doxo treatment alone. The combination of *p19-INK4D* induction and doxo treatment in IMR5/75 further increased the S phase fraction by 44.9-fold, indicating a prominent S phase block, and decreased the number of cells in G_2/M phase by 16.2-fold. In contrast, induction of *p16-INK4A* in combination with doxo treatment in IMR5/75 only slightly increased the $G_0/_1$ fraction, slightly decreased the G_2/M fraction, and did not alter the number of cells in the S phase (**Fig. 5C**). This implies that $p19^{INK4D}$ and $p16^{INK4A}$ act at least partly through different mechanisms to prevent accumulation of cells in G_2/M, with $p19^{INK4D}$ activating checkpoints during the G_1-S transition and S phase and $p16^{INK4A}$ activating only the G_1-S transition checkpoint. Intriguingly, the induction of *p19-INK4D*, but not *p16-INK4A*, sensitized *MYCN*-amplified IMR5/75, which has no additional alterations targeting the p53 pathway, for doxo-induced cell death (**Fig. 5D**).

Discussion

MYCN-amplified neuroblastoma cells show a distinct phenotype after drug-induced DNA damage. This is characterized by a failure to arrest in G_1-S, pronounced G_2/M cell enrichment and reduced cell death occurring equally in all phases of the cell cycle. We show that these changes are not only triggered by the higher MYCN dosage in these cells, but also by the genetic background of the tumor cells, specifically the additional chromosomal aberrations affecting p53 and pRB pathway members. Our results have also uncovered a novel function of MYCN in neuroblastoma cells that impairs a G_1-S arrest after drug-induced DNA damage through a mechanism other than the transcriptional suppression of p21 following p53 activation.

Our functional analyses of the CDK4/cyclin D-pRB axis indicate that high CDK4 kinase activity substantially contributes to impaired DNA damage-induced cell cycle arrest and cell death resistance in *MYCN*-amplified neuroblastoma cells. We show here that CDK4 inhibition restores G_1-S cell cycle arrest and reduces cell viability upon doxorubicin treatment in *MYCN*-amplified neuroblastoma cells. It was established earlier that almost all *MYCN*-amplified neuroblastoma cells with wild-type p53 fail to arrest at G_1-S despite p21 induction by different p53-activating stimuli, such as drug- or irradiation-induced DNA damage, $p14^{ARF}$ induction, or treatment with small compounds (e.g., nutlins) inhibiting the MDM2-p53 interaction.[12,23,27,43] In line with this, ectopic expression of p21 in neuroblastoma cells with amplified *MYCN* inhibits neither CDK2/cyclin E activity nor cell cycle progression.[28] Here, we demonstrate that high CDK4 activity is also causally involved in impaired DNA damage-induced cell cycle arrest in *MYCN*-amplified cells, at least in part by abrogating p21 function. In untreated neuroblastoma cells, we found that p21 is barely detectable in CDK4/cyclin D1 complexes, where it usually functions not only as an assembly factor for active CDK4/cyclin D1, but also as a cellular pool for p21 that can be quickly released upon DNA damage. It has been shown that DNA damage favors cyclin D1 proteolysis, thereby releasing p21 from the CDK4 complex, which, in turn, inhibits CDK2 and cell cycle progression.[35] Our data now indicate that a sufficient p21 reservoir is missing in *MYCN*-amplified neuroblastoma cells. Moreover, we found that upon drug-induced DNA damage, newly induced p21 is not only allocated to CDK2/cyclin E but also to CDK4/cyclin D1 complexes. Both complexes appear to compete for the newly synthesized p21, and an insufficient amount of p21 protein remains in complex with CDK2. The reduction in p21-bound CDK2 results in only a slight or no inhibitory effect on the overall CDK2 kinase activity in *MYCN*-amplified neuroblastoma cells (**Fig. 5E**). Accordingly, several MYCN-dependent and -independent mechanisms target p21 function in neuroblastoma cells: (1) transcriptional activation of *p21CIP1* is suppressed by abundant MYCN, which reduces the basal cellular p21 pool as well as the transcriptionally induced p21 following p53 activation;[23] (2) high abundance of CDK4/cyclin D1 complexes as a consequence of *CDK4*/*CCND1* gene amplification and/or transcriptional activation of CDK4 by MYCN; and (3) mutations altering p53 pathway functions.

We have also established that high CDK4 in *MYCN*-amplified cells has an unexpected function during S phase, promoting not only S phase progression, but also further cell death resistance.

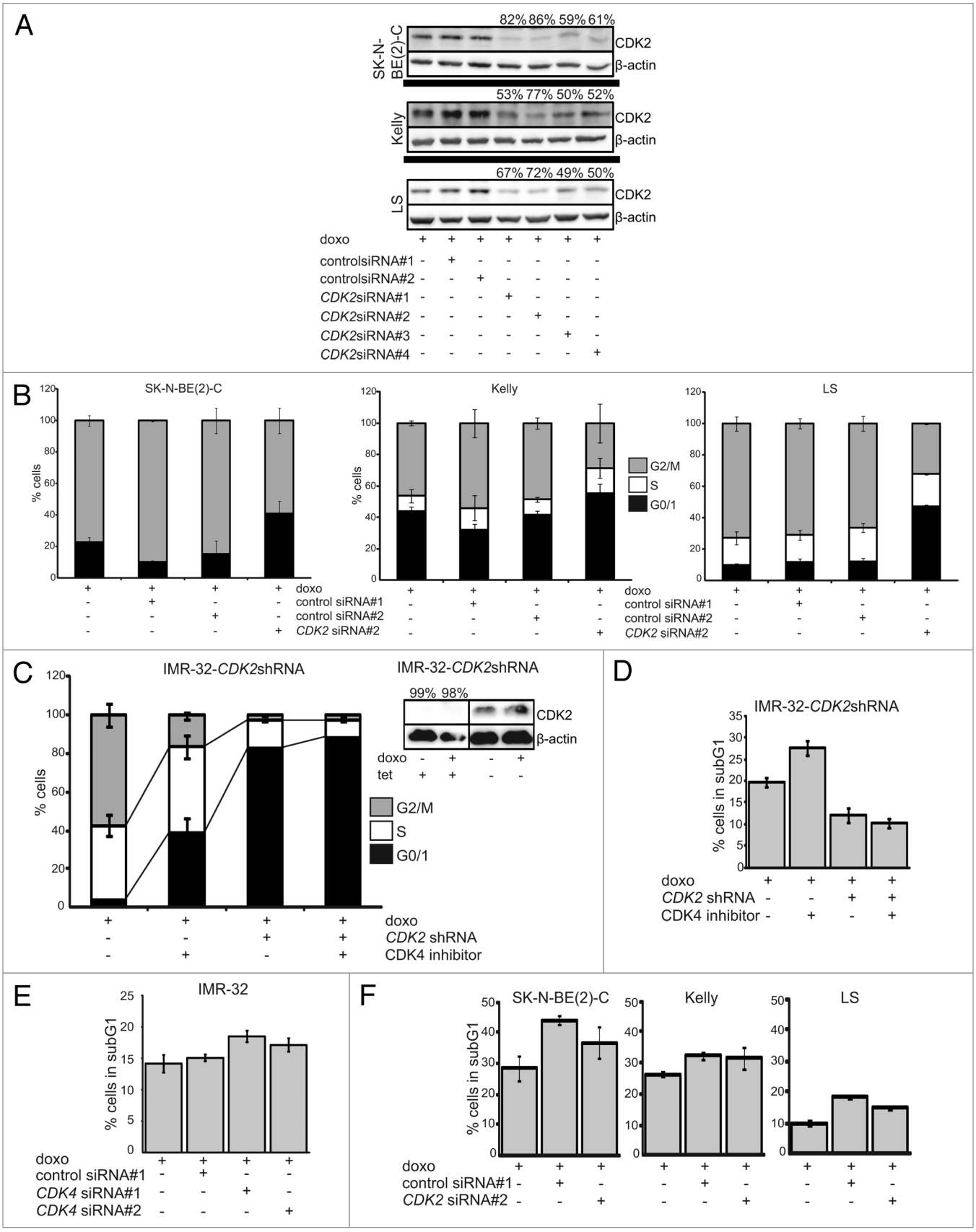

Figure 4. For figure legend, see page 1101.

Figure 4 (See opposite page). High CDK2 activity impairs drug-induced cell cycle arrest in *MYCN*-amplified neuroblastoma cells. Cells were transfected with one of four different *CDK2* siRNAs or one of two control siRNAs 24 h prior to doxo treatment. (**A**) Western blot showing the knockdown efficacies of the four *CDK2* siRNAs (%) and flow cytometric cell cycle analyses showing the *CDK2* siRNA#2 with highest knockdown efficacy 48 h after doxo treatment. (**C and D**) IMR-32 cells stably transfected with a tetracycline-inducible shRNA targeting *CDK2*. Addition of tetracycline to the culture medium induced expression of the *CDK2*-targeting shRNA. Cells were treated with doxo and/or the RO0505124 CDK4 inhibitor 24 h after shRNA induction. Cell cycle (**C**) and cell death (**D**) were analyzed using flow cytometry 48 h after treatment. (**E and F**) Cell death analysis for *MYCN*-amplified cells transiently transfected with two siRNAs targeting *CDK4* (**E**) or *CDK2* siRNA#2 (**F**). Cell death was determined using flow cytometry 48 h after doxo treatment. Data in (**B–F**) are presented as mean ± SD of triplicates.

CDK4 inhibition restored G_1-S cell cycle arrest associated with reduced cell viability and/or increased sensitivity to cell death in *MYCN*-amplified cells with or without additional alterations targeting p53 pathway components. S phase arrest and enhanced cell death after drug-induced DNA damage was not observed in the presence of *CDK2*-targeting siRNAs. Moreover, CDK2 inhibition reversed the chemosensitizing effect of CDK4 inhibition, probably through inhibiting G_1 to S transition. Single-strand DNA breaks may be tolerated in G_1 phase, but emerge to be more toxic as double-strand breaks during S phase.[44] CDK4 inhibition via $p19^{INK4D}$ or $p16^{INK4A}$ overexpression similarly delayed G_1-S transition in *MYCN*-amplified cells. However, $p19^{INK4D}$ but not $p16^{INK4A}$ overexpression in *MYCN*-amplified cells induced S phase arrest and had a modest chemosensitizing effect on cell death after drug-induced DNA damage, arguing for a specific function of $p19^{INK4D}$ during S phase.

Inhibitors specifically targeting CDK4/6 have been developed and shown to have antiproliferative effects on different cancer cell lines, including breast, ovarian, myeloma, mantle cell lymphoma, AML and glioblastoma cell models,[45-49] to prevent tumor growth in several human xenograft models[45,50,51] and are currently evaluated in phase I/II clinical trials.[52-55] Roberts et al. suggested that selective CDK4/6 inhibitors could be used in human cancers dependent on their CDK4/6 activity and sensitivity to chemotherapeutic drugs, either as antineoplastic agents to prevent myelosuppression, or for pharmacological synchronization, i.e., CDK4/6 inhibition synchronizes tumor cells to increase cell death by chemotherapeutic drugs in a cell cycle-dependent manner.[56] Since we showed that the higher MYCN dosage together with the cellular genetic background establishes the impaired DNA damage response in *MYCN*-amplified cells, combinatory treatment with CDK4 inhibitors and compounds leading to reduction of MYCN expression[57] may represent a potential therapeutic option in neuroblastoma. However, the effects of single or combined inhibition of cell cycle kinases, including CDK1, CDK2 and CDK4, in the context of drug-induced DNA damage response should be further investigated in vitro and in vivo using genetically well-defined neuroblastoma cell line and mouse models.

In conclusion, we demonstrate that the CDK4/cyclin D-pRB axis controls cell cycle progression after drug-induced DNA damage as an additional layer of control besides the p53-p21 axis in neuroblastoma cells. Furthermore, we have established that CDK4 inhibition sensitizes neuroblastoma cell lines with amplified *MYCN* and a deregulated p53/pRB pathway to the cytostatic effect of doxorubicin. This suggests that selective CDK4 inhibitors should be investigated more intensely as a potential future therapeutic option for neuroblastoma.

Materials and Methods

Cell culture. Cells were cultured as follows: SH-SY5Y and SK-N-BE(2)-C in DMEM; IMR-32, SH-EP, Kelly (*TP53* mutation),[58] IMR5/75, LS, TR14, NGP, SJ-NB-12, LA-N-5, LA-N-6, SK-N-AS and SK-N-MC (*EWS-FLi1* gene fusion)[59] in RPMI; both media were supplemented with 10% fetal calf serum. NB-7 were cultured in Neurobasal A-Medium containing 2% B27 supplement, 2 mM L-glutamine, 20 ng/ml rHuEGF, 20 ng/ml rHuFGFb and 2 μg/ml heparin. IMR5/75–6TR, used for tetracycline-inducible expression of $p16^{INK4A}$, $p19^{INK4D}$ or lacZ were cultured in RPMI supplemented with 10% fetal calf serum, 7.5 μg/ml blasticidin and 200 μg/ml G418. SH-EP-*MYCN* (TET21N), IMR5/75-C2 and IMR-32-*CDK2* shRNA were cultured and induced as previously described.[33,34,38] All neuroblastoma cell lines were analyzed using DNA fingerprinting by the "Deutsche Sammlung von Mikroorganismen und Zellkulturen" (DSMZ) in September 2008.

Plasmids. The human *p16-INK4A* or *p19-INK4D* open reading frame was cloned and transfected into IMR5/75-6TR, and the resulting clones were cultured and induced, as previously described.[60]

RNA interference. *CDK4* and *CDK2* siRNAs were obtained from Invitrogen Ltd. Validated Stealth RNAi DuoPak for *CDK4*, Duplex #1: 5'-GGG AGA UCA AGG UAA CCC UGG UGU U-3' and #2: 5'-GCG CCA GUU UCU AAG AGG CCU AGA U-3'; for *CDK2* Duplex #1: 5'-CCU UAA ACC UCA GAA UCU GCU UAU U-3' and #2: 5'-CCU AUU CCC UGG AGA UUC UGA GAU U-3'. *CDK2* siRNA #3 was designed as previously published.[38] *CDK2* siRNA #4 was designed to target *CDK2* on the same nucleotides as a previously described *CDK2* shRNA.[38] Silencer negative control #1 (AM4611) and #2 (AM4613) siRNAs were obtained from Ambion. Cells were seeded into 6-well plates for flow cytometry or 10-cm^2 plates for western blotting and transfected using Lipofectamine 2000 (Invitrogen) according to the manufacturers' protocol.

Immunoprecipitation. Cells were plated in 15-cm^2 plates and lysed in 1,000 μl RIPA buffer (50 mM Tris-HCL pH 7.4, 1% NP-40, 0.25% Na-deoxycholate, 1 mM EDTA, two protease inhibitor tablets; see Millipore protocol), and 500 μg of protein was immunoprecipitated with 2 μg of the specific antibody bound to Dynabeads Protein G (Invitrogen). Bound proteins were eluted by boiling in SDS-sample buffer and then resolved on 12.5% SDS-PAGE. Antibodies were used as previously published.[35]

In vitro CDK1, CDK2 or CDK4 kinase assay. To determine CDK1, CDK2 or CDK4 activity, specific complexes were immunoprecipitated as described above. Kinase activity was

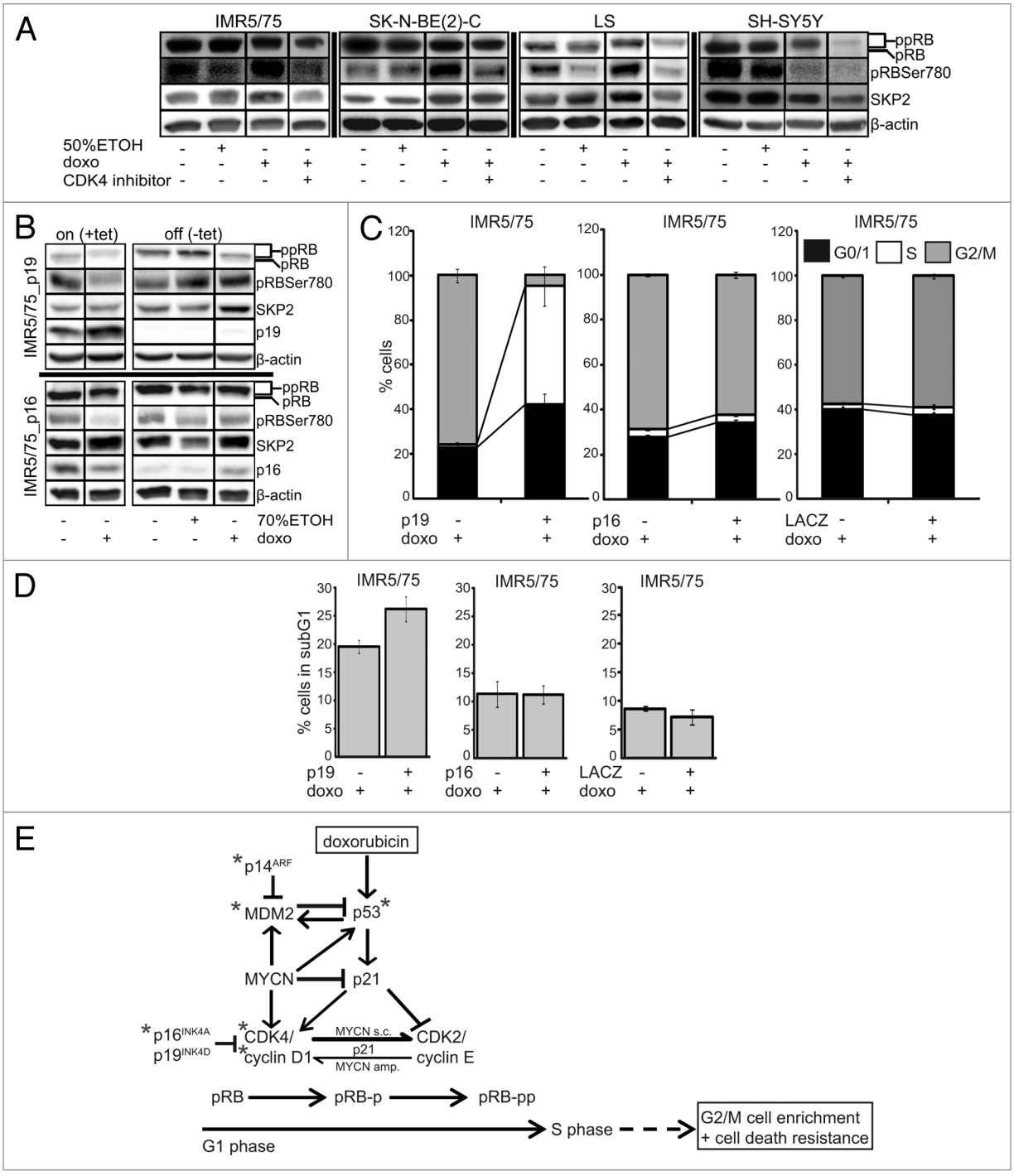

Figure 5. *p19*^{INK4D}, but not *p16*^{INK4A}, abrogates CDK4-mediated pRB phosphorylation and cell cycle progression in *MYCN*-amplified neuroblastoma cells and sensitizes for cell death after drug-induced DNA damage. (**A**) Western blot of whole-cell protein extracts 48 h after treatment with doxo and/or the CDK4 inhibitor, RO0505124. Since RO0505124 was dissolved in 50% ethanol, we used this as control. Tetracycline (tet), dissolved in 70% ethanol, was added to the culture medium of IMR5/75 cells to induce *p19-INK4D* (= p19+), *p16-INK4A* (= p16+) or *lacZ*. Doxo was added to the culture medium 48 h after induction. 70% ethanol was used as control. Western blot (**B**) and flow cytometric analyses of the cell cycle (**C**) or cell death (**D**) were performed 48 h after doxo treatment. IMR5/75 cells stably transfected with a tetracycline-inducible *lacZ* construct were used as control and showed neither cell cycle distribution nor cell death fraction changes upon induction of *lacZ* in untreated and doxo-treated cultures. Flow cytometry data are presented as mean ± SD of triplicates. (**E**) Schematic model of doxorubicin-induced DNA damage response in neuroblastoma cells. Note: *, genetic aberrations; s.c., single-copy; amp., amplified; pRB, hypophosphorylated; pRB-p, partially phosphorylated; pRB-pp, hyperphosphorylated.

analyzed using the ADP-Glo Kinase Assay Kit (Promega), the CDK2/Cyclin A2 or CDK1/Cyclin A2 Kinase Enzyme System (Promega) or RB substrate (upstate cell signaling solutions) following the manufactures' instructions. Luminescence was assessed using the FLUOstar Optima microplate fluorescence reader (BMG LABTECH).

Protein expression. Whole-cell lysates were prepared and protein expression visualized as previously described.[61] Fifty μg of protein lysate was separated per lane on 7–15% SDS-PAGE. Blots were probed with antibodies directed against Phospho-RB Ser780 (#9307, Cell Signaling Technology), RB (#554136, BD Biosciences), CDK2 (#09550, Dianova), CDK4 (#09583, Dianova), cyclinD1 (#08330, Dianova), p21 (#sc-6246, Santa Cruz), p53 (#sc-126, Santa Cruz), SKP2 (#08-1334, Zymed Laboratories Inc.), p19 (#sc-56334, Santa Cruz), p16 (#sc-9968, Santa Cruz) or β-actin (#A5441, Sigma-Aldrich). HSR-peroxidase-labeled anti-mouse (#115-035-003, Dianova) or anti-rabbit (#111-035-144, Dianova) antibodies were used as secondary antibodies.

Viability assay. Cells were seeded at 5,000 cells per well in 96-well plates and primed with RO0505124 24 h later. Four hours later, doxorubicin was added to the culture medium. AlamarBlue assay (ABD Serotec) was performed according to the manufacturer's instructions. Fluorescence was detected using the FluoStar Optima microplate fluorescence reader (BMG LABTECH).

Flow cytometric analysis of cell cycle and cell death. Cells were plated in 25-cm^2 flasks or 6-well plates. Flow cytometry was used to assess cell cycle and cell death as previously described.[62] The APOBrdU Kit (Phoenix Flow Systems) was used to detect BrdU-positive cells according to the manufacturers' protocol.

(Multicolor) fluorescence in situ hybridization (FISH/mFISH). FISH was performed to analyze the status of *CCND1* in each cell line using BAC DNA probes (RP11-554A11 and RP11-614E9) labeled with FITC (Molecular Probes) or Cy3 (GE Healthcare) coupled dUTPs by nick translation as previously described.[63] Normal lymphocytes were used as control cells to ensure the correct signal number and position of BAC clones. mFISH was performed as previously published.[63]

Pharmacological inhibition. Cell cultures were treated with 0.1 μg/ml doxorubicin (TOC-2252-M010, Biozol) and 2.5 μM RO0505124 (Roche) where indicated.

Disclosure of Potential Conflicts of Interest

No potential conflicts of interest were disclosed.

Acknowledgments

We thank J.J. Molenaar for providing the IMR-32 cell line carrying an inducible *CDK2* shRNA and K. Astrahantseff for manuscript editing. Financial support was provided as follows: BMBF, NGFN^{Plus} #01GS0896 (L.M. Brueckner, L. Savelyeva, F. Westermann); European Union (EU, FP6), EET-Pipeline (#037260, D. Dreidax, S. Gogolin, F. Westermann); EU (FP7), ASSET (#259348-2, D. Dreidax, S. Gogolin, F. Westermann); Helmholtz-Russia Joint Research Groups, HRJRG-006 (L.M. Brueckner, L. Savelyeva); EU Marie-Curie-Fellowship, E. Bell.

Supplemental Materials

Supplemental materials may be found here:
www.landesbioscience.com/journals/cc/article/24091

References

1. D'Angio GJ, Evans AE, Koop CE. Special pattern of widespread neuroblastoma with a favourable prognosis. Lancet 1971; 1:1046-9; PMID:4102970; http://dx.doi.org/10.1016/S0140-6736(71)91606-0
2. Haas D, Ablin AR, Miller C, Zoger S, Matthay KK. Complete pathologic maturation and regression of stage IVS neuroblastoma without treatment. Cancer 1988; 62:818-25; PMID:3293764; http://dx.doi.org/10.1002/1097-0142(19880815)62:4<818::AID-CNCR2820620430>3.0.CO;2-K
3. Evans AE, Gerson J, Schnaufer L. Spontaneous regression of neuroblastoma. Natl Cancer Inst Monogr 1976; 44:49-54; PMID:1030781
4. De Bernardi B, Nicolas B, Boni L, Indolfi P, Carli M, Cordero Di Montezemolo L, et al.; Italian Co-Operative Group for Neuroblastoma. Disseminated neuroblastoma in children older than one year at diagnosis: comparable results with three consecutive high-dose protocols adopted by the Italian Co-Operative Group for Neuroblastoma. J Clin Oncol 2003; 21:1592-601; PMID:12697885; http://dx.doi.org/10.1200/JCO.2003.05.191
5. Matthay KK, Villablanca JG, Seeger RC, Stram DO, Harris RE, Ramsay NK, et al.; Children's Cancer Group. Treatment of high-risk neuroblastoma with intensive chemotherapy, radiotherapy, autologous bone marrow transplantation, and 13-cis-retinoic acid. N Engl J Med 1999; 341:1165-73; PMID:10519894; http://dx.doi.org/10.1056/NEJM199910143411601
6. Zage PE, Kletzel M, Murray K, Marcus R, Castleberry R, Zhang Y, et al.; Children's Oncology Group. Outcomes of the POG 9340/9341/9342 trials for children with high-risk neuroblastoma: a report from the Children's Oncology Group. Pediatr Blood Cancer 2008; 51:747-53; PMID:18704922; http://dx.doi.org/10.1002/pbc.21713
7. Seeger RC, Brodeur GM, Sather H, Dalton A, Siegel SE, Wong KY, et al. Association of multiple copies of the N-myc oncogene with rapid progression of neuroblastomas. N Engl J Med 1985; 313:1111-6; PMID:4047115; http://dx.doi.org/10.1056/NEJM198510313131802
8. Brodeur GM, Seeger RC, Schwab M, Varmus HE, Bishop JM. Amplification of N-myc in untreated human neuroblastomas correlates with advanced disease stage. Science 1984; 224:1121-4; PMID:6719137; http://dx.doi.org/10.1126/science.6719137
9. Fulda S, Lutz W, Schwab M, Debatin KM. MycN sensitizes neuroblastoma cells for drug-induced apoptosis. Oncogene 1999; 18:1479-86; PMID:10050884; http://dx.doi.org/10.1038/sj.onc.1202435
10. Lutz W, Fulda S, Jeremias I, Debatin KM, Schwab M. MycN and IFNgamma cooperate in apoptosis of human neuroblastoma cells. Oncogene 1998; 17:339-46; PMID:9690515; http://dx.doi.org/10.1038/sj.onc.1200201
11. Paffhausen T, Schwab M, Westermann F. Targeted MYCN expression affects cytotoxic potential of chemotherapeutic drugs in neuroblastoma cells. Cancer Lett 2007; 250:17-24; PMID:17141950; http://dx.doi.org/10.1016/j.canlet.2006.09.010
12. Bell E, Premkumar R, Carr J, Lu X, Lovat PE, Kees UR, et al. The role of MYCN in the failure of MYCN amplified neuroblastoma cell lines to G1 arrest after DNA damage. Cell Cycle 2006; 5:2639-47; PMID:17172827; http://dx.doi.org/10.4161/cc.5.22.3443
13. Chen L, Iraci N, Gherardi S, Gamble LD, Wood KM, Perini G, et al. p53 is a direct transcriptional target of MYCN in neuroblastoma. Cancer Res 2010; 70:1377-88; PMID:20145147; http://dx.doi.org/10.1158/0008-5472.CAN-09-2598
14. Knudsen KE, Booth D, Naderi S, Sever-Chroneos Z, Fribourg AF, Hunton IC, et al. RB-dependent S-phase response to DNA damage. Mol Cell Biol 2000; 20:7751-63; PMID:11003670; http://dx.doi.org/10.1128/MCB.20.20.7751-7763.2000
15. Mayhew CN, Perkin LM, Zhang X, Sage J, Jacks T, Knudsen ES. Discrete signaling pathways participate in RB-dependent responses to chemotherapeutic agents. Oncogene 2004; 23:4107-20; PMID:15064736; http://dx.doi.org/10.1038/sj.onc.1207503
16. Harrington EA, Bruce JL, Harlow E, Dyson N. pRB plays an essential role in cell cycle arrest induced by DNA damage. Proc Natl Acad Sci USA 1998; 95:11945-50; PMID:9751770; http://dx.doi.org/10.1073/pnas.95.20.11945
17. Brugarolas J, Moberg K, Boyd SD, Taya Y, Jacks T, Lees JA. Inhibition of cyclin-dependent kinase 2 by p21 is necessary for retinoblastoma protein-mediated G1 arrest after gamma-irradiation. Proc Natl Acad Sci USA 1999; 96:1002-7; PMID:9927683; http://dx.doi.org/10.1073/pnas.96.3.1002
18. Lowe SW, Bodis S, McClatchey A, Remington L, Ruley HE, Fisher DE, et al. p53 status and the efficacy of cancer therapy in vivo. Science 1994; 266:807-10; PMID:7973635; http://dx.doi.org/10.1126/science.7973635
19. Carr-Wilkinson J, O'Toole K, Wood KM, Challen CC, Baker AG, Board JR, et al. High Frequency of p53/MDM2/p14ARF Pathway Abnormalities in Relapsed Neuroblastoma. Clin Cancer Res 2010; 16:1108-18; PMID:20145180; http://dx.doi.org/10.1158/1078-0432.CCR-09-1865
20. Bell E, Chen L, Liu T, Marshall GM, Lunec J, Tweddle DA. MYCN oncoprotein targets and their therapeutic potential. Cancer Lett 2010; 293:144-57; PMID:20153925; http://dx.doi.org/10.1016/j.canlet.2010.01.015

21. Tweddle DA, Pearson AD, Haber M, Norris MD, Xue C, Flemming C, et al. The p53 pathway and its inactivation in neuroblastoma. Cancer Lett 2003; 197:93-8; PMID:12880966; http://dx.doi.org/10.1016/S0304-3835(03)00088-0
22. Carr-Wilkinson J, Griffiths R, Elston R, Gamble LD, Goranov B, Redfern CP, et al. Outcome of the p53-mediated DNA damage response in neuroblastoma is determined by morphological subtype and MYCN expression. Cell Cycle 2011; 10:3778-87; PMID:22052359; http://dx.doi.org/10.4161/cc.10.21.17973
23. Eckerle I, Muth D, Batzler J, Henrich KO, Lutz W, Fischer M, et al. Regulation of BIRC5 and its isoform BIRC5-2B in neuroblastoma. Cancer Lett 2009; 285:99-107; PMID:19497660; http://dx.doi.org/10.1016/j.canlet.2009.05.007
24. Westermann F, Muth D, Benner A, Bauer T, Henrich KO, Oberthuer A, et al. Distinct transcriptional MYCN/c-MYC activities are associated with spontaneous regression or malignant progression in neuroblastomas. Genome Biol 2008; 9:R150; PMID:18851746; http://dx.doi.org/10.1186/gb-2008-9-10-r150
25. Slack A, Chen Z, Tonelli R, Pule M, Hunt L, Pession A, et al. The p53 regulatory gene MDM2 is a direct transcriptional target of MYCN in neuroblastoma. Proc Natl Acad Sci USA 2005; 102:731-6; PMID:15644444; http://dx.doi.org/10.1073/pnas.0405495102
26. He J, Gu L, Zhang H, Zhou M. Crosstalk between MYCN and MDM2-p53 signal pathways regulates tumor cell growth and apoptosis in neuroblastoma. Cell Cycle 2011; 10:2994-3002; PMID:21862876; http://dx.doi.org/10.4161/cc.10.17.17118
27. McKenzie PP, Guichard SM, Middlemas DS, Ashmun RA, Danks MK, Harris LC. Wild-type p53 can induce p21 and apoptosis in neuroblastoma cells but the DNA damage-induced G1 checkpoint function is attenuated. Clin Cancer Res 1999; 5:4199-207; PMID:10632361
28. McKenzie PP, Danks MK, Kriwacki RW, Harris LC. P21Waf1/Cip1 dysfunction in neuroblastoma: a novel mechanism of attenuating G0-G1 cell cycle arrest. Cancer Res 2003; 63:3840-4; PMID:12839982
29. Tweddle DA, Malcolm AJ, Cole M, Pearson AD, Lunec J. p53 cellular localization and function in neuroblastoma: evidence for defective G(1) arrest despite WAF1 induction in MYCN-amplified cells. Am J Pathol 2001; 158:2067-77; PMID:11395384; http://dx.doi.org/10.1016/S0002-9440(10)64678-0
30. Keshelava N, Seeger RC, Groshen S, Reynolds CP. Drug resistance patterns of human neuroblastoma cell lines derived from patients at different phases of therapy. Cancer Res 1998; 58:5396-405; PMID:9850071
31. Gewirtz DA. A critical evaluation of the mechanisms of action proposed for the antitumor effects of the anthracycline antibiotics adriamycin and daunorubicin. Biochem Pharmacol 1999; 57:727-41; PMID:10075079; http://dx.doi.org/10.1016/S0006-2952(98)00307-4
32. Rouaud P, Fiancette R, Vincent-Fabert C, Magnone V, Cogné M, Dubus P, et al. Mantle cell lymphoma-like lymphomas in c-myc-3'RR/p53+/– mice and c-myc-3'RR/Cdk4R24C mice: differential oncogenic mechanisms but similar cellular origin. Oncotarget 2012; 3:586-93; PMID:22592113
33. Muth D, Ghazaryan S, Eckerle I, Beckett E, Pöhler C, Batzler J, et al. Transcriptional repression of SKP2 is impaired in MYCN-amplified neuroblastoma. Cancer Res 2010; 70:3791-802; PMID:20424123; http://dx.doi.org/10.1158/0008-5472.CAN-09-1245
34. Lutz W, Stöhr M, Schürmann J, Wenzel A, Löhr A, Schwab M. Conditional expression of N-myc in human neuroblastoma cells increases expression of alpha-prothymosin and ornithine decarboxylase and accelerates progression into S-phase early after mitogenic stimulation of quiescent cells. Oncogene 1996; 13:803-12; PMID:8761302
35. Agami R, Bernards R. Distinct initiation and maintenance mechanisms cooperate to induce G1 cell cycle arrest in response to DNA damage. Cell 2000; 102:55-66; PMID:10929713; http://dx.doi.org/10.1016/S0092-8674(00)00010-6
36. Burgess A, Wigan M, Giles N, Depinto W, Gillespie P, Stevens F, et al. Inhibition of S/G2 phase CDK4 reduces mitotic fidelity. J Biol Chem 2006; 281:9987-95; PMID:16476733; http://dx.doi.org/10.1074/jbc.M512714200
37. Wohlbold L, Merrick KA, De S, Amat R, Kim JH, Larochelle S, et al. Chemical genetics reveals a specific requirement for Cdk2 activity in the DNA damage response and identifies Nbs1 as a Cdk2 substrate in human cells. PLoS Genet 2012; 8:e1002935; PMID:22927831; http://dx.doi.org/10.1371/journal.pgen.1002935
38. Molenaar JJ, Ebus ME, Geerts D, Koster J, Lamers F, Valentijn LJ, et al. Inactivation of CDK2 is synthetically lethal to MYCN over-expressing cancer cells. Proc Natl Acad Sci USA 2009; 106:12968-73; PMID:19525400; http://dx.doi.org/10.1073/pnas.0901418106
39. Kitagawa M, Higashi H, Jung HK, Suzuki-Takahashi I, Ikeda M, Tamai K, et al. The consensus motif for phosphorylation by cyclin D1-Cdk4 is different from that for phosphorylation by cyclin A/E-Cdk2. EMBO J 1996; 15:7060-9; PMID:9003781
40. Serrano M, Hannon GJ, Beach D. A new regulatory motif in cell-cycle control causing specific inhibition of cyclin D/CDK4. Nature 1993; 366:704-7; PMID:8259215; http://dx.doi.org/10.1038/366704a0
41. Chan FK, Zhang J, Cheng L, Shapiro DN, Winoto A. Identification of human and mouse p19, a novel CDK4 and CDK6 inhibitor with homology to p16ink4. Mol Cell Biol 1995; 15:2682-8; PMID:7739548
42. Guan KL, Jenkins CW, Li Y, O'Keefe CL, Noh S, Wu X, et al. Isolation and characterization of p19INK4d, a p16-related inhibitor specific to CDK6 and CDK4. Mol Biol Cell 1996; 7:57-70; PMID:8741839
43. Gogolin S, Dreidax D, Becker G, Ehemann V, Schwab M, Westermann F. MYCN/MYC-mediated drug resistance mechanisms in neuroblastoma. Int J Clin Pharmacol Ther 2010; 48:489-91; PMID:20557856
44. Johnson SM, Torrice CD, Bell JF, Monahan KB, Jiang Q, Wang Y, et al. Mitigation of hematologic radiation toxicity in mice through pharmacological quiescence induced by CDK4/6 inhibition. J Clin Invest 2010; 120:2528-36; PMID:20577054; http://dx.doi.org/10.1172/JCI41402
45. Baughn LB, Di Liberto M, Wu K, Toogood PL, Louie T, Gottschalk R, et al. A novel orally active small molecule potently induces G1 arrest in primary myeloma cells and prevents tumor growth by specific inhibition of cyclin-dependent kinase 4/6. Cancer Res 2006; 66:7661-7; PMID:16885367; http://dx.doi.org/10.1158/0008-5472.CAN-06-1098
46. Finn RS, Dering J, Conklin D, Kalous O, Cohen DJ, Desai AJ, et al. PD 0332991, a selective cyclin D kinase 4/6 inhibitor, preferentially inhibits proliferation of luminal estrogen receptor-positive human breast cancer cell lines in vitro. Breast Cancer Res 2009; 11:R77; PMID:19874578; http://dx.doi.org/10.1186/bcr2419
47. Konecny GE, Winterhoff B, Kolarova T, Qi J, Manivong K, Dering J, et al. Expression of p16 and retinoblastoma determines response to CDK4/6 inhibition in ovarian cancer. Clin Cancer Res 2011; 17:1591-602; PMID:21278246; http://dx.doi.org/10.1158/1078-0432.CCR-10-2307
48. Marzec M, Kasprzycka M, Lai R, Gladden AB, Wlodarski P, Tomczak E, et al. Mantle cell lymphoma cells express predominantly cyclin D1a isoform and are highly sensitive to selective inhibition of CDK4 kinase activity. Blood 2006; 108:1744-50; PMID:16690963; http://dx.doi.org/10.1182/blood-2006-04-016634
49. Wang L, Wang J, Blaser BW, Duchemin AM, Kusewitt DF, Liu T, et al. Pharmacologic inhibition of CDK4/6: mechanistic evidence for selective activity or acquired resistance in acute myeloid leukemia. Blood 2007; 110:2075-83; PMID:17537993; http://dx.doi.org/10.1182/blood-2007-02-071266
50. Fry DW, Harvey PJ, Keller PR, Elliott WL, Meade M, Trachet E, et al. Specific inhibition of cyclin-dependent kinase 4/6 by PD 0332991 and associated antitumor activity in human tumor xenografts. Mol Cancer Ther 2004; 3:1427-38; PMID:15542782
51. Michaud K, Solomon DA, Oermann E, Kim JS, Zhong WZ, Prados MD, et al. Pharmacologic inhibition of cyclin-dependent kinases 4 and 6 arrests the growth of glioblastoma multiforme intracranial xenografts. Cancer Res 2010; 70:3228-38; PMID:20354191; http://dx.doi.org/10.1158/0008-5472.CAN-09-4559
52. Flaherty KT, Lorusso PM, Demichele A, Abramson VG, Courtney R, Randolph SS, et al. Phase I, dose-escalation trial of the oral cyclin-dependent kinase 4/6 inhibitor PD 0332991, administered using a 21-day schedule in patients with advanced cancer. Clin Cancer Res 2012; 18:568-76; PMID:22090362; http://dx.doi.org/10.1158/1078-0432.CCR-11-0509
53. Leonard JP, LaCasce AS, Smith MR, Noy A, Chirieac LR, Rodig SJ, et al. Selective CDK4/6 inhibition with tumor responses by PD0332991 in patients with mantle cell lymphoma. Blood 2012; 119:4597-607; PMID:22383795; http://dx.doi.org/10.1182/blood-2011-10-388298
54. Schwartz GK, LoRusso PM, Dickson MA, Randolph SS, Shaik MN, Wilner KD, et al. Phase I study of PD 0332991, a cyclin-dependent kinase inhibitor, administered in 3-week cycles (Schedule 2/1). Br J Cancer 2011; 104:1862-8; PMID:21610706; http://dx.doi.org/10.1038/bjc.2011.177
55. www.clinicaltrials.gov/ct2/results?/term=PD-0332991
56. Roberts PJ, Bisi JE, Strum JC, Combest AJ, Darr DB, Usary JE, et al. Multiple roles of cyclin-dependent kinase 4/6 inhibitors in cancer therapy. J Natl Cancer Inst 2012; 104:476-87; PMID:22302033; http://dx.doi.org/10.1093/jnci/djs002
57. Sottile F, Gnemmi I, Cantilena S, D'Acunto WC, Sala A. A chemical screen identifies the chemotherapeutic drug topotecan as a specific inhibitor of the B-MYB/MYCN axis in neuroblastoma. Oncotarget 2012; 3:535-45; PMID:22619121
58. Horvilleur E, Bauer M, Goldschneider D, Mergui X, de la Motte A, Bénard J, et al. p73alpha isoforms drive opposite transcriptional and post-transcriptional regulation of MYCN expression in neuroblastoma cells. Nucleic Acids Res 2008; 36:4222-32; PMID:18583365; http://dx.doi.org/10.1093/nar/gkn394
59. Dunn T, Praissman L, Hagag N, Viola MV. ERG gene is translocated in an Ewing's sarcoma cell line. Cancer Genet Cytogenet 1994; 76:19-22; PMID:8076344; http://dx.doi.org/10.1016/0165-4608(94)90063-9
60. Henrich KO, Bauer T, Schulte J, Ehemann V, Deubzer H, Gogolin S, et al. CAMTA1, a 1p36 tumor suppressor candidate, inhibits growth and activates differentiation programs in neuroblastoma cells. Cancer Res 2011; 71:3142-51; PMID:21385898; http://dx.doi.org/10.1158/0008-5472.CAN-10-3014
61. Afanasyeva EA, Mestdagh P, Kumps C, Vandesompele J, Ehemann V, Theissen J, et al. MicroRNA miR-885-5p targets CDK2 and MCM5, activates p53 and inhibits proliferation and survival. Cell Death Differ 2011; 18:974-84; PMID:21233845; http://dx.doi.org/10.1038/cdd.2010.164
62. Ehemann V, Hashemi B, Lange A, Otto HF. Flow cytometric DNA analysis and chromosomal aberrations in malignant glioblastomas. Cancer Lett 1999; 138:101-6; PMID:10378780; http://dx.doi.org/10.1016/S0304-3835(98)00383-8
63. Brueckner LM, Sagulenko E, Hess EM, Zheglo D, Blumrich A, Schwab M, et al. Genomic rearrangements at the FRA2H common fragile site frequently involve non-homologous recombination events across LTR and L1(LINE) repeats. Hum Genet 2012; 131:1345-59; PMID:22476624; http://dx.doi.org/10.1007/s00439-012-1165-3